On the optimal CFL number of SSP methods for hyperbolic problems

Andrew Giuliani[a], Lilia Krivodonova[a,*]

[a]*Department of Applied Mathematics, University of Waterloo*

Abstract

We show that the theory for strong stability preserving (SSP) time stepping methods employed with the method of lines-type discretizations of hyperbolic conservation laws may result in overly stringent time step restrictions. We analyze a fully discrete finite volume method with slope reconstruction and a second order SSP Runge-Kutta time integrator to show that the maximum stable time step can be increased over the SSP limit. Numerical examples show that this result extends to two-dimensional problems on triangular meshes.

1. Introduction

In one dimension, hyperbolic conservation laws are of the form

$$\frac{\partial u}{\partial t} + \frac{\partial}{\partial x} f(u) = 0, \tag{1}$$

where $u(x,t)$ is the solution and $f(u)$ is the flux function. A popular approach to solving these partial differential equations (PDEs) is the method of lines. This entails first discretizing the spatial derivative, e.g., with the finite volume (FV) method. The result is said to be in a semidiscrete form and is a system of ordinary differential equations (ODEs) for the degrees of freedom (DOFs) of the spatial discretization

$$\frac{d}{dt} U = L(U), \tag{2}$$

where U is the numerical solution which approximates u and the operator L approximates $-\frac{\partial}{\partial x} f(u)$. This system is then advanced in time using a time stepping scheme, e.g., an explicit Runge-Kutta (RK) method. Typically, one chooses a time integrator of the same order as the spatial order of accuracy. If $L(U)$ is linear, then stability of the fully discrete scheme under a suitable time step restriction can be shown using the

*Corresponding author
Email address: lgk@uwaterloo.ca (Lilia Krivodonova)

absolute stability region of the time stepper and the eigenvalues of the spatial operator L [1, 2, 3]. This approach cannot be directly applied if $L(U)$ is nonlinear, e.g., if $f(u)$ is nonlinear or if $f(u)$ is linear but a limiter is applied. In this case, we can first show stability of a forward Euler time step applied to (2), i.e.,

$$||U + \Delta t L(U)|| \leq ||U||, \quad \forall U, \tag{3}$$

where $\Delta t \leq \Delta t_{\text{FE}}$ and Δt_{FE} is the maximum stable forward Euler time step specific to the chosen spatial discretization and $||\cdot||$ is a convex functional [4]. This result can be extended to a higher order RK method if it can be written as a convex combination of forward Euler time steps. If each forward Euler step does not violate the stability property, then a convex combination of them will not either. This is the idea behind strong stability preserving (SSP) methods [5, 6, 7]. The need for these time discretizations was demonstrated in [8, 9, 10]. If the high-order time stepper is not SSP, then an oscillation-free numerical solution is not guaranteed even if the spatial reconstruction is total variation diminishing.

The time step Δt of high-order SSP methods is related to Δt_{FE} by the SSP coefficient c [10], i.e.,

$$\Delta t \leq c \Delta t_{\text{FE}}. \tag{4}$$

The optimal SSP coefficient for the second and third order RK methods, SSP-RK2 and SSP-RK3, is $c = 1$, meaning that forward Euler, RK2, and RK3 time integrators all have the same severe time step restriction. For example, second order finite volume methods with linear slope reconstruction (Section 3) coupled with the forward Euler method have a CFL number of $\frac{1}{2}$, i.e., $\Delta t_{FE} = \frac{1}{2}\frac{h}{a}$. Thus, by the standard SSP theory, this spatial discretization coupled with the SSP-RK2 and SSP-RK3 methods also have a CFL number of $\frac{1}{2}$. In two dimensions, this maximum allowable CFL number becomes $\frac{1}{6}$, i.e., $\Delta t_{FE} = \frac{1}{6}\frac{h}{||\mathbf{a}||}$, for the discontinuous Galerkin (DG) method coupled with the vertex-based limiter in [11]. This is unlike what is known about linear stability of RK methods, where increasing the number of stages in the RK time stepper can increase the area of its absolute stability region and possibly increase the maximum stable time step.

The advantage of using the standard SSP analysis is that from the stability of the spatial discretization coupled with the forward Euler method, stability with high-order SSP time integrators is guaranteed under the suitable time step restriction (4). This time step restriction may or may not be tight. We show that by analyzing the fully discrete FV and RK2 schemes, the SSP coefficient in (4) can be increased while still guaranteeing stability of the numerical solution in the maximum norm. We note that our analysis does

not preclude the existence of spatial discretizations for which (4) is tight.

It has been shown in other contexts that the SSP restriction (4) can be relaxed without sacrificing positivity of the solution, in e.g. [12, 13] for well resolved and smooth problems. Additionally, if monotonicity in an inner product norm rather than in a convex functional is desired then a more relaxed time step restriction than (4) is possible [14]. The work presented here makes no assumptions on the solution and shows that the maximum stable time step of a second order finite volume scheme can be increased by analyzing the fully discrete spatial and temporal discretization.

2. The FV method

We consider a second order finite volume method with slope reconstruction. The periodic computational domain is divided uniformly into elements Ω_i with left, $x_{i-\frac{1}{2}}$, and right, $x_{i+\frac{1}{2}}$, end points, where $h = x_{i+\frac{1}{2}} - x_{i-\frac{1}{2}}$ is the grid spacing. A semi-discrete finite volume scheme for (1) is given by

$$\frac{d}{dt}U_i = \frac{1}{h}\left[f^*(Q_{i-1}(x_{i-\frac{1}{2}}), Q_i(x_{i-\frac{1}{2}})) - f^*(Q_i(x_{i+\frac{1}{2}}), Q_{i+1}(x_{i+\frac{1}{2}}))\right], \tag{5}$$

where U_i is an approximation to the cell average of the exact solution on Ω_i, $Q_i(x)$ is a linearly reconstructed solution on Ω_i, and f^* is the numerical flux [15]. The linearly reconstructed numerical solution at time t^n on cell Ω_i is

$$Q_i^n(x) = U_i^n + \sigma_i^n(x - x_i) \text{ for } x \in [x_{i-\frac{1}{2}}, x_{i+\frac{1}{2}}]. \tag{6}$$

The slope σ_i^n is reconstructed using a second order TVD limiter [16, 17]. Using (6), we define the correction term

$$\Delta_i^n = U_{i,r}^n - U_i^n = U_i^n - U_{i,l}^n, \tag{7}$$

where $U_{i,r}^n = Q_i^n(x_{i+\frac{1}{2}})$ and $U_{i,l}^n = Q_i^n(x_{i-\frac{1}{2}})$. With a TVD limiter, we have

$$\Delta_{i-1}^n = \gamma_{i-\frac{1}{2},l}(U_i^n - U_{i-1}^n) \text{ and } \Delta_i^n = \gamma_{i-\frac{1}{2},r}(U_i^n - U_{i-1}^n), \tag{8}$$

for $0 \le \gamma_{i-\frac{1}{2},l}, \gamma_{i-\frac{1}{2},r} \le 1$ (Figure 1). Assuming a linear flux $f(u) = au$ where $a > 0$, and the upwind numerical flux in (5), we obtain the scheme

$$\frac{d}{dt}U_i = \frac{1}{h}(aU_{i-1,r} - aU_{i,r}). \tag{9}$$

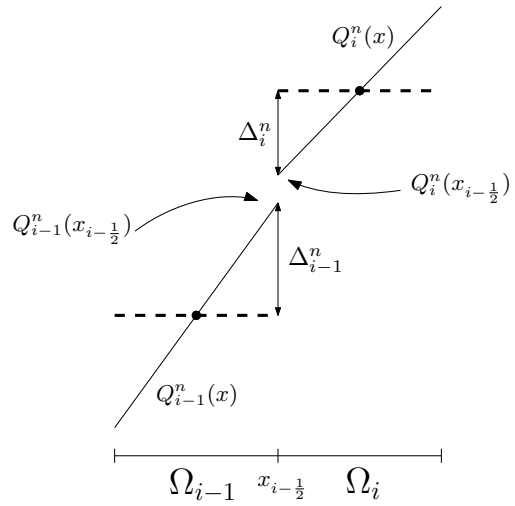

Figure 1: Cell averages (dashed lines) and reconstructed slopes (solid lines).

Adding and subtracting aU_i inside the parentheses on the right-hand-side of (9), we have

$$\frac{d}{dt}U_i = \frac{a}{h}(U_{i-1,r} - U_i) - \frac{a}{h}(U_{i,r} - U_i). \tag{10}$$

Substituting the second identity of (7) into (10), we obtain

$$\frac{d}{dt}U_i = \frac{a}{h}(U_{i-1,r} - U_i) - \frac{a}{h}(U_i - U_{i,l}). \tag{11}$$

3. First order forward Euler time stepping

We discretize (11) in time using the forward Euler method to obtain a second order in space finite volume scheme, which has been examined in [10, 15, 18]. This gives

$$U_i^{n+1} = \left(1 - 2\Delta t\frac{a}{h}\right) U_i^n + \Delta t\frac{a}{h}U_{i-1,r}^n + \Delta t\frac{a}{h}U_{i,l}^n. \tag{12}$$

Letting $\alpha = 2\Delta t\frac{a}{h}$, the cell average at t^{n+1} becomes

$$U_i^{n+1} = (1-\alpha)\, U_i^n + \frac{\alpha}{2}U_{i-1,r}^n + \frac{\alpha}{2}U_{i,l}^n.$$

When using a reconstruction (6) with a TVD slope limiter, $U_{i-1,r}^n, U_{i,l}^n$ will lie within the interval defined by the cell averages of Ω_i's neighbors (Figure 1). Clearly, if $\alpha \leq 1$, then U_i^{n+1} can be expressed as a convex combination of solution values at t^n, and the scheme (12) will be stable in the maximum norm. Thus, the

forward Euler time step restriction is

$$\Delta t_{FE} \leq \frac{1}{2}\frac{h}{a}.$$

4. Second order Runge-Kutta time stepping

The first and second intermediate solution values of the RK2 time stepping algorithm can be written as

$$U_i^{(1)} = (1-\alpha)\, U_i^n + \frac{\alpha}{2} U_{i-1,r}^n + \frac{\alpha}{2} U_{i,l}^n, \tag{13}$$

$$U_i^{(2)} = (1-\alpha)\, U_i^{(1)} + \frac{\alpha}{2} U_{i-1,r}^{(1)} + \frac{\alpha}{2} U_{i,l}^{(1)}. \tag{14}$$

On each cell, the left $U_{i,l}^{(1)}$ and right $U_{i,r}^{(1)}$ intermediate values can be written in terms of the average $U_i^{(1)}$ and the correction term $\Delta_i^{(1)}$

$$U_{i,l}^{(1)} = U_i^{(1)} - \Delta_i^{(1)} \text{ and } U_{i,r}^{(1)} = U_i^{(1)} + \Delta_i^{(1)}. \tag{15}$$

Substituting $U_i^n = (U_{i,l}^n + U_{i,r}^n)/2$ into (13), and (15) into (14), the RK2 algorithm becomes

$$U_i^{(1)} = \frac{1-\alpha}{2}\left(U_{i,l}^n + U_{i,r}^n\right) + \frac{\alpha}{2} U_{i-1,r}^n + \frac{\alpha}{2} U_{i,l}^n, \tag{16}$$

$$U_i^{(2)} = (1-\alpha)\, U_i^{(1)} + \frac{\alpha}{2}\left(U_{i-1}^{(1)} + \Delta_{i-1}^{(1)}\right) + \frac{\alpha}{2}\left(U_i^{(1)} - \Delta_i^{(1)}\right), \tag{17}$$

$$U_i^{n+1} = \frac{U_i^{(2)} + U_i^n}{2}. \tag{18}$$

Substituting (16) and (17) into (18) yields

$$U_i^{n+1} = \left(-\frac{1}{8}\alpha + \frac{1}{2}\right) U_{i,l}^n + \frac{1}{8}\alpha U_{i-1,l}^n + \left(-\frac{1}{4}\alpha^2 + \frac{3}{8}\alpha\right) U_{i-1,r}^n + \frac{1}{8}\alpha^2 U_{i-2,r}^n + \left(\frac{1}{8}\alpha^2 - \frac{3}{8}\alpha + \frac{1}{2}\right) U_{i,r}^n + \frac{1}{4}\alpha(\Delta_{i-1}^{(1)} - \Delta_i^{(1)}).$$

U_i^{n+1} is now in terms of the solution values at t^n and the correction terms $\Delta_i^{(1)}$ and $\Delta_{i-1}^{(1)}$. From (8), the values of $\Delta_i^{(1)}$ and $\Delta_{i-1}^{(1)}$ take on the following four extreme cases:

1. $\Delta_i^{(1)} = 0$ and $\Delta_{i-1}^{(1)} = 0$,
2. $\Delta_i^{(1)} = U_i^{(1)} - U_{i-1}^{(1)}$ and $\Delta_{i-1}^{(1)} = U_i^{(1)} - U_{i-1}^{(1)}$,
3. $\Delta_i^{(1)} = 0$ and $\Delta_{i-1}^{(1)} = U_i^{(1)} - U_{i-1}^{(1)}$,

4. $\Delta_i^{(1)} = U_i^{(1)} - U_{i-1}^{(1)}$ and $\Delta_{i-1}^{(1)} = 0$.

For each of the above cases, we will show that U_i^{n+1} can be written as a convex combination of solution values at t^n, i.e.,

$$U_i^{n+1} = \sum_j d_j U_j, \tag{19}$$

where U_j are understood to be solution averages at time t^n or values at the left and right endpoints of the elements. The multipliers d_j, which are functions of α, must satisfy the following conditions

1. Sum condition

$$\sum_j d_j = 1, \tag{20}$$

2. Positivity condition

$$d_j \geq 0 \qquad \forall j, \tag{21}$$

in order for the scheme to preserve the local and global bounds on the solution. In each of the Cases 1-4, the sum condition (20) is satisfied. We will now comment on the values of α for which the multipliers d_j are nonnegative.

Cases 1. and 2.

$$U_i^{n+1} = \left(-\frac{1}{8}\alpha + \frac{1}{2}\right) U_{i,l}^n + \frac{1}{8}\alpha U_{i-1,l}^n + \left(-\frac{1}{4}\alpha^2 + \frac{3}{8}\alpha\right) U_{i-1,r}^n + \frac{1}{8}\alpha^2 U_{i-2,r}^n + \left(\frac{1}{8}\alpha^2 - \frac{3}{8}\alpha + \frac{1}{2}\right) U_{i,r}^n.$$

The multipliers are positive for $0 \leq \alpha \leq \frac{3}{2}$.

Case 3.

$$U_i^{n+1} = \frac{1}{2} U_{i,l}^n + \frac{1}{4}\alpha U_{i-1,r}^n + \left(-\frac{1}{4}\alpha + \frac{1}{2}\right) U_{i,r}^n.$$

The multipliers are positive for $0 \leq \alpha \leq 2$.

Case 4.

$$U_i^{n+1} = \frac{1}{2}\left(1 - \frac{1}{2}\alpha\right) U_{i,l}^n + \frac{1}{2}\left(1 - \alpha + \frac{1}{2}\alpha^2\right) U_{i,r}^n + \frac{1}{4}\alpha U_{i-1,l}^n + \frac{1}{2}\left(\alpha - \alpha^2\right) U_{i-1,r}^n + \frac{1}{4}\alpha^2 U_{i-2,r}^n.$$

The multipliers in the above expression are nonnegative for $0 \leq \alpha \leq 1$. We can obtain a larger interval for α by rearranging terms. Introducing the difference $\left(U_{i-1,l}^n - U_{i-1,r}^n\right)$ and using $U_i^n = (U_{i,l}^n + U_{i,r}^n)/2$, we

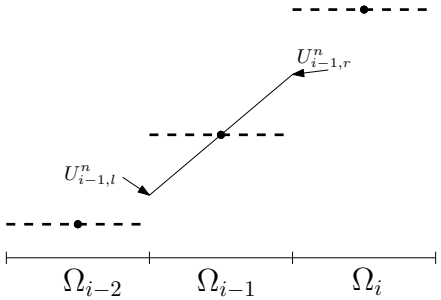

Figure 2: The limiter ensures that $U_{i-1,l} - U_{i-1,r} = \beta(U_{i-2} - U_i)$, where $0 \le \beta \le 1$.

obtain

$$U_i^{n+1} = \left(1 - \frac{1}{2}\alpha\right) U_i^n + \frac{1}{4}\left(\alpha^2 - \alpha\right) U_{i,r}^n + \left(-\frac{1}{2}\alpha^2 + \frac{3}{4}\alpha\right) U_{i-1,l}^n + \frac{1}{2}\left(\alpha^2 - \alpha\right)\left(U_{i-1,l}^n - U_{i-1,r}^n\right) + \frac{1}{4}\alpha^2 U_{i-2,r}^n.$$

With a limiter, the solution satisfies

$$U_{i-1,l}^n - U_{i-1,r}^n = \beta\left(U_{i-2}^n - U_i^n\right)$$

for some $0 \le \beta \le 1$ (Figure 2). Then, the scheme can be written as

$$U_i^{n+1} = \left(-\frac{1}{2}\beta\alpha^2 + \frac{1}{2}(\beta - 1)\alpha + 1\right) U_i^n + \frac{1}{2}\beta\left(\alpha^2 - \alpha\right) U_{i-2}^n + \left(\frac{3}{4}\alpha - \frac{1}{2}\alpha^2\right) U_{i-1,l}^n + \frac{1}{4}\alpha^2 U_{i-2,r}^n + \frac{1}{4}(\alpha^2 - \alpha) U_{i,r}^n. \tag{22}$$

The multipliers are positive for

$$1 \le \alpha \le \sqrt{2}.$$

Combining this interval with $0 \le \alpha \le 1$, we obtain with this expression for U_i^{n+1} that it can be written as a convex combination of solution values at t^n with $0 \le \alpha \le \sqrt{2}$, though we need to use two different expressions.

A slightly larger bound on α can be obtained if we specify which TVD slope limiter is used in the scheme. For example, consider the monotonized central-difference (MC) slope limiter [19]

$$\sigma_i^n = \frac{1}{h}\text{minmod}\left(2(U_i^n - U_{i-1}^n), \frac{U_{i+1}^n - U_{i-1}^n}{2}, 2(U_{i+1}^n - U_i^n)\right). \tag{23}$$

With this limiter, we now show that $0 \le \beta \le \frac{1}{2}$. First, assume that the forward, central, and backward differences are all of the same sign and nonzero. Then, multiplying both sides of (23) by $h/(U_{i+1}^n - U_{i-1}^n)$,

recognizing that $U_{i,r}^n - U_{i,l}^n = h\sigma_i^n$, and substituting $\beta = (U_{i,r}^n - U_{i,l}^n)/(U_{i+1}^n - U_{i-1}^n)$, we have

$$\beta = \min\left(2\frac{U_i^n - U_{i-1}^n}{U_{i+1}^n - U_{i-1}^n}, \frac{1}{2}, 2\frac{U_{i+1}^n - U_i^n}{U_{i+1}^n - U_{i-1}^n}\right).$$

From the above, it is clear that β is bounded above by $\frac{1}{2}$. If the forward, central, and backward differences do not have the same sign or at least one is zero, then $\beta = 0$. This gives that $0 \leq \beta \leq \frac{1}{2}$. From this smaller interval for the β coefficient, we have that the multipliers of (22) are positive for

$$1 \leq \alpha \leq \frac{3}{2}.$$

Combining this interval with $0 \leq \alpha \leq 1$, we obtain that this expression for U_i^{n+1} can be written as a convex combination of solution values at t^n with $0 \leq \alpha \leq \frac{3}{2}$.

Putting it all together.

Combining the above with the results from Section 3, we find that the scheme satisfies the local maximum principle for $0 \leq \alpha \leq \sqrt{2}$. All above cases are convex combinations of solution values at time t^n, thus a larger time step than in (4) is possible. The time step restriction is therefore

$$\Delta t \leq \frac{\sqrt{2}}{2}\frac{h}{a}. \tag{24}$$

Taking into account the chosen TVD limiter, which in our case is the MC limiter, this time step restriction can be increased to

$$\Delta t \leq \frac{3}{4}\frac{h}{a}. \tag{25}$$

Remark

These results are based on the assumption of a piecewise linear numerical solution and a limiter that forces solution values to belong to a local interval defined by its immediate neighbors. As such, this larger CFL number immediately extends to other spatial discretizations, e.g. the DG method, where we have stability of the solution means in the maximum norm.

N	Error	Minimum	Maximum
25	2.814176e-01 (-)	-8.019780e-01	8.042554e-01
50	1.072674e-01 (1.39)	-9.306829e-01	9.283151e-01
100	3.476506e-02 (1.62)	-9.748830e-01	9.748830e-01
200	9.814755e-03 (1.82)	-9.906997e-01	9.906997e-01
400	2.629868e-03 (1.89)	-9.965111e-01	9.965111e-01
800	6.910883e-04 (1.92)	-9.986542e-01	9.986542e-01

Table 1: L_1 errors, rates of convergence (in parentheses), and global minimum and maximum of cell averages with the number of cells N for Example 5.1.

N	Minimum	Maximum
25	1.912839e-04	9.994733e-01
50	8.725729e-09	1
100	0	1
200	0	1
400	0	1
800	0	1

Table 2: Global minimum and maximum of cell averages in terms of the number of elements in Example 5.2.

5. Numerical examples

In this section, we demonstrate that numerical solutions obtained with the time step restriction (25) and the MC limiter are accurate and stable. Unless otherwise stated, in all one-dimensional examples we use periodic boundary conditions on the domain $[-1, 1]$ and integrate until the final time $T = 1$.

5.1. Advecting sine wave

We solve (1) with the flux $f(u) = u$ and the initial condition $u_0(x) = \cos(2\pi x)$. We provide the L_1 errors, convergence rates, and lower and upper bounds attained by the solution means in Table 1. We observe that the scheme is second order accurate and preserves the global minimum and maximum of the solution.

5.2. Advecting discontinuities

We solve (1) with the flux $f(u) = u$ and the initial condition $u_0(x) = 1$ if $x < 0,$ and 0 elsewhere. The exact and numerical solutions at the final time are plotted in Figure 3. The global minimum and maximum of the cell averages are maintained. We tabulate them at the final time in Table 2.

5.3. Euler equations

We solve the Sod tube problem on the domain $[0, 1]$ with the initial states $(\rho_l, u_l, p_l) = (1, 0, 1)$ and $(\rho_r, u_r, p_r) = (0.125, 0, 0.1)$ to the left and right of $x = 0.5$, respectively. The exact and numerical solutions

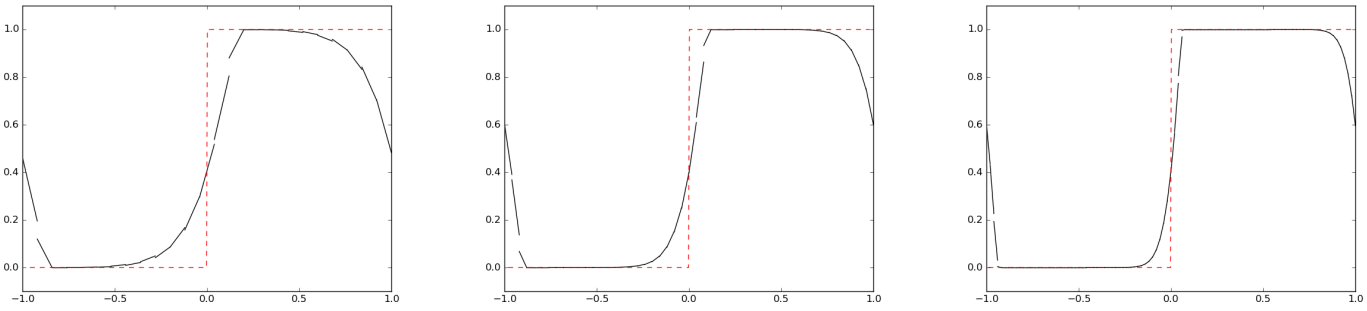

(a) $N = 25$ (b) $N = 50$ (c) $N = 100$

Figure 3: Exact (dashed line) and numerical (solid line) solutions (Example 5.2).

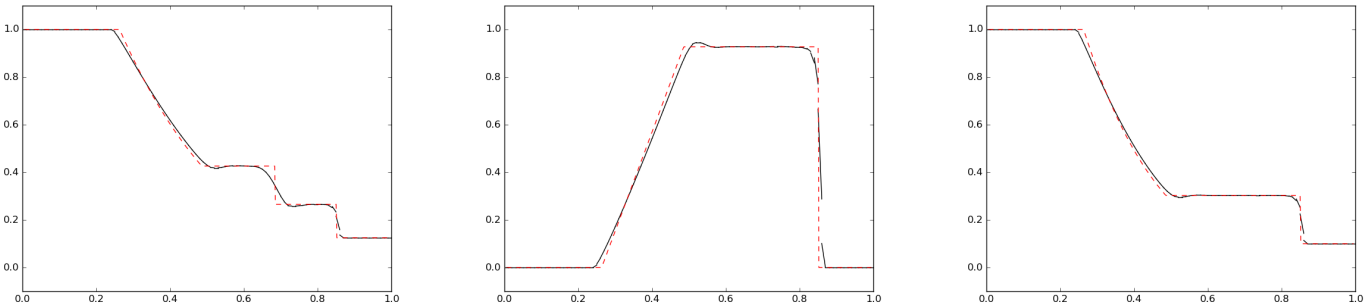

(a) Density (b) Velocity (c) Pressure

Figure 4: Exact (dashed) and numerical (solid) density, velocity, and pressure for the Sod tube problem with $N = 100$ (Example 5.3).

at the final time $T = 0.2$ are plotted in Figure 4; slight over- and undershoots are observed in the numerical solution. These oscillations are due to the reconstruction in conserved variables [20] and are present when the CFL number is both $\frac{3}{4}$ and $\frac{1}{2}$. These overshoots and undershoots can occur even in numerical solutions obtained with first order schemes, e.g., Godunov's method, [21, 22].

5.4. Two-dimensional advection equation

In this example, we demonstrate that a larger time step is possible in two dimensions, as well as with a spatial discretization different from the FV method. We solve $u_t + u_x + u_y = 0$ on $[-1, 1]^2$ using the DG spatial discretization with a linear basis, coupled with the limiter based on the vertex neighborhood in [11]. The mesh was obtained by discretizing the domain into a 40×40 grid of squares, then splitting each square along its diagonal from the top left to bottom right, into two triangles. It was shown in [11] that solution means do not grow in the maximum norm when

$$\Delta t \leq \text{CFL} \frac{h}{||\mathbf{a}||}, \tag{26}$$

1/CFL	Minimum	Maximum
3	-9.50e-18	1.000336
4	-6.15e-18	1
5	-3.93e-18	1
6	**-3.62e-18**	**1**

Table 3: Minimum and maximum cell averages for Example 5.4 using time step restriction (26) for various CFL numbers.

with CFL $\leq \frac{1}{6}$, $\mathbf{a}$ being the direction of flow, and h being the cell width in the direction of $\mathbf{a}$. Here, $h = \frac{1}{40}\sqrt{2}$. The problem is solved until a final time $T = 0.1$ with the initial condition $u_0(x, y) = 1$ if $\max(|x|, |y|) \leq \frac{1}{4}$, and 0 elsewhere.

In Table 3, we show the global maximum and minimum cell averages over the entire mesh for various CFL numbers. Extrapolating from the one-dimensional analysis, we see that the numerical solution in two dimensions preserves the global bounds on the solution for a time step $\Delta t \leq \frac{3}{2}\Delta t_{\text{FE}} = \frac{1}{4}\frac{h}{||\mathbf{a}||}$.

6. Conclusion

We have demonstrated analytically and numerically for one-dimensional finite volume methods that the time step restriction for the stability in the maximum norm with RK2 time stepping is larger than the SSP theory's prediction. We provide numerical evidence that this conclusion extends to two dimensions and other spatial discretizations, e.g., the DG method. The main conclusion here is that the strong stability of the fully discrete numerical method depends on both the temporal and spatial discretizations. We believe that the result can be extended to other SSP methods and spatial discretization schemes. The analysis in multi-dimensions and for time integrators using a larger number of stages will be significantly more involved algebraically.

7. Acknowledgment

This work was supported in part by the Natural Sciences and Engineering Research Council of Canada grant 341373-07, and an Alexander Graham Bell PGS-D grant. We gratefully acknowledge the support of the NVIDIA Corporation with the donation of hardware used for this research.

[1] L. Krivodonova and R. Qin, "An analysis of the spectrum of the discontinuous Galerkin method," *Applied Numerical Mathematics*, vol. 64, no. Supplement C, pp. 1 – 18, 2013.

[2] L. Krivodonova and R. Qin, "An analysis of the spectrum of the discontinuous Galerkin method II: Nonuniform grids," *Applied Numerical Mathematics*, vol. 71, pp. 41–62, 2013.

[3] N. Chalmers and L. Krivodonova, "Spatial and modal superconvergence of the discontinuous Galerkin method for linear equations," *Journal of Scientific Computing*, vol. 72, pp. 128–146, Jul 2017.

[4] S. Gottlieb, D. Ketcheson, and C.-W. Shu, *Strong Stability Preserving Runge-Kutta and Multistep Time Discretizations*. River Edge, NJ, USA: World Scientific Publishing Co., Inc., 2011.

[5] D. I. Ketcheson, "Highly efficient strong stability preserving Runge-Kutta methods with low-storage implementations," *SIAM Journal on Scientific Computing*, vol. 30, no. 4, pp. 2113–2136, 2008.

[6] S. Gottlieb, "On high order strong stability preserving Runge-Kutta and multi step time discretizations," *Journal of Scientific Computing*, vol. 25, no. 1, pp. 105–128, 2005.

[7] S. Gottlieb, C.-W. Shu, and E. Tadmor, "Strong stability-preserving high-order time discretization methods," *SIAM review*, vol. 43, no. 1, pp. 89–112, 2001.

[8] C.-W. Shu, "Total-variation-diminishing time discretizations," *SIAM J. Sci. Stat. Comput.*, vol. 9, pp. 1073–1084, Nov. 1988.

[9] C.-W. Shu and S. Osher, "Efficient implementation of essentially non-oscillatory shock-capturing schemes," *Journal of Computational Physics*, vol. 77, no. 2, pp. 439 – 471, 1988.

[10] S. Gottlieb and C.-W. Shu, "Total variation diminishing Runge-Kutta schemes," *Mathematics of computation of the American Mathematical Society*, vol. 67, no. 221, pp. 73–85, 1998.

[11] A. Giuliani and L. Krivodonova, "Analysis of slope limiters on unstructured meshes of triangles," *Preprint at* `http://www.math.uwaterloo.ca/~agiulian/GIULIANI_limiters.pdf`, 2017.

[12] Z. Horvàth, "On the positivity step size threshold of Runge-Kutta methods," *Applied Numerical Mathematics*, vol. 53, no. 2, pp. 341 – 356, 2005. Tenth Seminar on Numerical Solution of Differential and Differntial-Algebraic Euqations (NUMDIFF-10).

[13] Z. Horvàth, "On the positivity of matrix-vector products," *Linear Algebra and its Applications*, vol. 393, pp. 253 – 258, 2004. Special Issue on Positivity in Linear Algebra.

[14] I. Higueras, "Monotonicity for Runge-Kutta methods: Inner product norms," *Journal of Scientific Computing*, vol. 24, pp. 97–117, Jul 2005.

[15] R. J. LeVeque, *Finite Volume Methods for Hyperbolic Problems*. Cambridge University Press, 2002.

[16] P. K. Sweby, "High resolution schemes using flux limiters for hyperbolic conservation laws," *SIAM Journal on Numerical Analysis*, vol. 21, no. 5, pp. 995–1011, 1984.

[17] M. Berger, M. Aftosmis, and S. Muman, "Analysis of slope limiters on irregular grids," in *43rd AIAA Aerospace Sciences Meeting and Exhibit*, p. 490, 2005.

[18] B. van Leer, "Towards the ultimate conservative difference scheme. V. A second-order sequel to Godunov's method," *Journal of Computational Physics*, vol. 32, no. 1, pp. 101 – 136, 1979.

[19] B. Van Leer, "Towards the ultimate conservative difference scheme. IV. A new approach to numerical convection," *Journal of Computational Physics*, vol. 23, no. 3, pp. 276–299, 1977.

[20] B. Cockburn, S.-Y. Lin, and C.-W. Shu, "TVB Runge-Kutta local projection discontinuous Galerkin finite element method for conservation laws III: one-dimensional systems," *Journal of Computational Physics*, vol. 84, no. 1, pp. 90–113, 1989.

[21] E. F. Toro, *Riemann solvers and numerical methods for fluid dynamics: a practical introduction*. Springer Science & Business Media, 2013.

[22] S. Karni and S. Čanić, "Computations of slowly moving shocks," *Journal of Computational Physics*, vol. 136, no. 1, pp. 132–139, 1997.